Prospects of searches for neutral, long-lived particles that decay to photons using timing at CDF

David Toback* and Peter Wagner†

Texas A&M University, College Station, Texas 77843-4242, USA

(Received 3 July 2004; published 22 December 2004)

We present the prospects of searches for neutral, long-lived particles that decay to photons using their time of arrival measured with a newly installed timing system on the electromagnetic calorimeter (EMTiming) of the Collider Detector at Fermilab (CDF). A Monte Carlo simulation shows that EMTiming can provide separation between decay photons from neutral, long-lived particles and prompt photons from standard model backgrounds. Using gauge mediated supersymmetry breaking (GMSB) $\tilde{\chi}_1^0 \to \gamma\tilde{G}$ models, we estimate a quasi-model-independent sensitivity using only direct neutralino pair production, and also estimate the expected 95% confidence level exclusion regions for all superpartner production as a function of the neutralino mass and lifetime. We find that a combination of single photon and diphoton analyses should allow the Tevatron in Run II to easily extend the exclusion regions from ALEPH at LEP II at high neutralino masses and lifetimes, and cover parts of the theoretically favored $m_{\tilde{G}} <$ few keV$/c^2$ GMSB parameter space.

DOI: 10.1103/PhysRevD.70.114032 PACS numbers: 13.85.Rm, 13.85.Qk, 14.80.–j, 14.80.Ly

I. INTRODUCTION

The electromagnetic (EM) calorimeter at the Collider Detector at Fermilab (CDF) [1] has recently been equipped with a new nanosecond-resolution timing system, EMTiming [2], to measure the arrival time of energy deposited (e.g., from photons). While it was initially designed to reject cosmics and accelerator backgrounds [3], we investigate the possibility of using it to search for neutral particles [4] with a lifetime of the order of a nanosecond that decay in flight to photons. An example of a theory that would produce these particles is gauge mediated supersymmetry breaking (GMSB) [5] with a neutralino, $\tilde{\chi}_1^0$, as the next-to-lightest supersymmetric particle (NLSP) and a light gravitino, $\tilde{G}$, as the LSP. In this scenario, the neutralino decays preferably ($\sim 100\%$) as $\tilde{\chi}_1^0 \to \gamma\tilde{G}$ with a macroscopic lifetime for much of the GMSB parameter space. We study the phenomenology and the prospects of searches for events that contain long-lived particles producing time-delayed photons, and show what an analysis using a timing system in the EM calorimeter might look like.

Decay photons from long-lived particles as in GMSB/supersymmetry will have a later arrival time than prompt photons produced from standard model (SM) sources. A suitable separation variable is

$$\Delta s \equiv (t_f - t_i) - \frac{|\vec{x}_f - \vec{x}_i|}{c}, \tag{1}$$

where $t_f - t_i$ is the time between the collision and the arrival time of the photon, and $|\vec{x}_f - \vec{x}_i|$ is the distance between the final position of the photon and the collision point. Prompt (SM) photons will produce $\Delta s = 0$ and photons from long-lived particles $\Delta s > 0$, for perfect measurements. The situation is visualized in Fig. 1. All four variables can be measured by the CDF detector [6] with a system resolution of $\sigma_{\Delta s} \sim 1.0$ ns [7]. See Appendix A for details.

We estimate the sensitivity to two different types of new particle production using GMSB models. As a quasi-model-independent sensitivity estimate to generic long-lived particles, we simulate direct neutralino pair production and decay. For a "full" GMSB model sensitivity

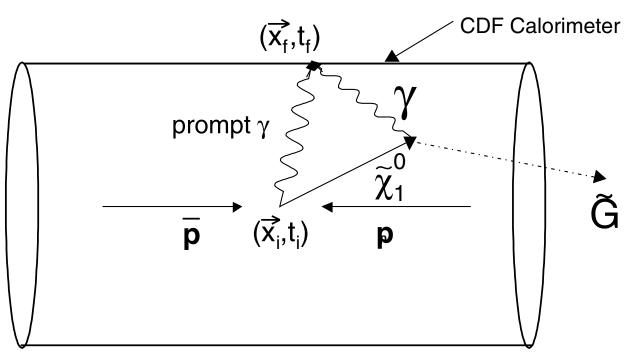

FIG. 1. A schematic diagram of a long-lived neutralino decaying to a photon and a gravitino in the CDF detector. The neutralino emanates from the collision at $(\vec{x}_i, t_i)$ and after a time τ it decays. While the gravitino leaves the detector, the photon travels to the detector wall and deposits energy in the EM calorimeter where its final location $\vec{x}_f$ and arrival time t_f can be measured. A prompt photon would travel directly from $\vec{x}_i$ to $\vec{x}_f$. The difference between the actual time the neutralino/photon needs, $\Delta t = t_f - t_i$, and the time a prompt photon would need, $|\vec{x}_f - \vec{x}_i|/c$, is defined as Δs. The SM typically produces prompt photons which have $\Delta s = 0$ ns, whereas photons from delayed decays from SUSY have $\Delta s > 0$ ns, assuming a perfect measurement.

*Electronic address: toback@fnal.gov
†Electronic address: wagnp@fnal.gov

estimate, which means including all relevant GMSB subprocesses such that the neutralinos are part of cascades from gauginos and squarks, we allow all SUSY particle production and decay. For both we examine the dependency on neutralino mass, $m_{\tilde{\chi}}$, and lifetime, $\tau_{\tilde{\chi}}$.

To choose analysis final states we consider three issues: (1) With neutralino lifetimes longer than a nanosecond, one or both of the neutralinos can leave the detector before they decay; (2) gravitinos or the neutralino leaving the detector provide missing transverse energy, $\not\!\!E_T$; (3) to ensure that background predictions are as reliable as possible, we want to use the data selection requirements from previously published papers by CDF [1] and D0 [8]. In the 1992–1995 collider run of the Tevatron (Run I), three types of analyses match these criteria: CDF and D0 results in $\gamma\gamma + \not\!\!E_T$ [3,9], exclusive $\gamma + \not\!\!E_T$ ($\gamma + \not\!\!E_T + 0$ jets) from CDF [10], and $\gamma + \not\!\!E_T + \geq 2$ jets ($\gamma + \not\!\!E_T +$ jets) from D0 [11]. In direct neutralino pair production, we consider analyses with final states $\gamma\gamma + \not\!\!E_T$ and $\gamma + \not\!\!E_T + 0$ jets as there are no parton-level jets. For full GMSB neutralino production from cascade decays, we consider both $\gamma\gamma + \not\!\!E_T$ and $\gamma + \not\!\!E_T +$ jets analyses.

We quantify the sensitivity for 2 fb^{-1} luminosity using the expected 95% confidence level (C.L.) cross section upper limits, as that is a conservative estimate for the integrated luminosity at the end of Run II. Results for both with and without the EMTiming system, using kinematics cuts only, illustrate the contribution to the final sensitivity from kinematic and timing information considerations [12]. Finally, we compare the final mass and lifetime exclusion regions for a certain GMSB model line to direct and indirect searches from the ALEPH experiment at LEP II [13] and to favored cosmological regions [14].

Before we proceed further, we note that this study is designed to answer the question of whether timing methods can provide sufficient separation between signal and SM backgrounds. The feasibility of such an analysis depends critically on the ability to efficiently identify photons which do not arrive at the face of the detector at the usual 90° incident angle. This would require a full detector simulation which is beyond the scope of this paper and should be done separately for any collaboration wishing to use these results. For the purpose of this study, we assume that this issue can be addressed without significant changes to the identification efficiency, as was done at ALEPH [13]. We further assume that the additional handles such as EMTiming and timing in the hadronic calorimeters provide the necessary robustness needed to convince ourselves that photons which might not pass ordinary selection requirements are indeed from the signal source as opposed to sources which could produce fake photons and $\not\!\!E_T$, like cosmics.

II. NEUTRALINO PAIR PRODUCTION AS A MEASURE OF QUASI-MODEL-INDEPENDENT SENSITIVITY

A. Analysis methods and their efficiency as a function of neutralino mass and lifetime

To estimate the sensitivity to neutral, long-lived particles which decay to photons in as model-independent a manner

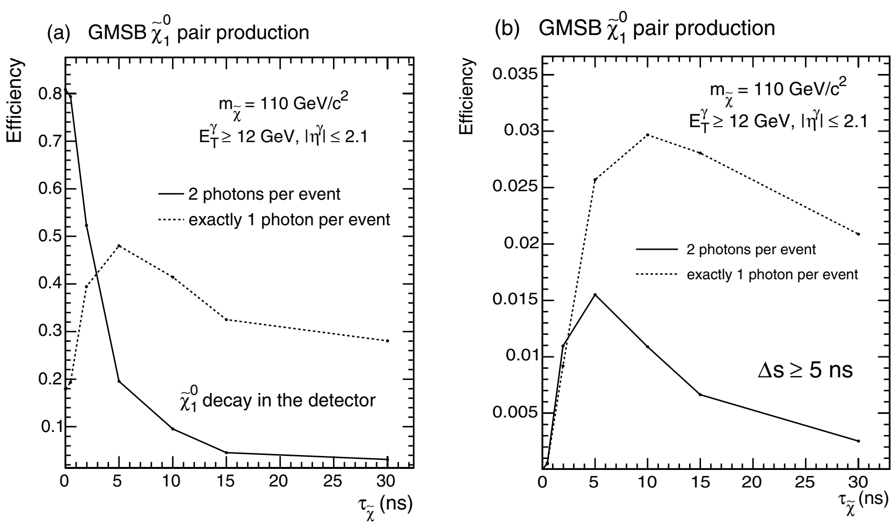

FIG. 2. The efficiency for events to pass the various Δs cuts as a function of the neutralino lifetime at $m_{\tilde{\chi}} = 110$ GeV$/c^2$. The results are separated into single and diphoton events for which the neutralino decays in the detector, and for $\Delta s \geq 5.0$ ns. For any Δs restriction above 0, the efficiency approaches zero at $\tau_{\tilde{\chi}} = 0$ ns, since all photons ideally have $\Delta s = 0$ ns. For high τ, neutralinos have a higher probability to leave the detector. For any Δs requirement, one can find an efficiency maximum at about 5–10 ns. Single photon events have higher efficiency towards higher Δs requirements and/or higher lifetimes, due to increasing probability for a photon to leave the detector. Thus, we expect a $\gamma\gamma + \not\!\!E_T$ to provide the best sensitivity for very low lifetimes, and a $\gamma + \not\!\!E_T$ analysis to be best for higher lifetimes.

as possible, we consider a GMSB model [15] which we restrict to direct neutralino pair production and decay: $p\bar{p} \to \tilde{\chi}_1^0\tilde{\chi}_1^0 \to \gamma\tilde{G}\gamma\tilde{G}$. We use the PYTHIA [16] event generator, with ISAJET [17] to generate the SUSY masses, and PGS with the parameter file for the CDF detector [18] as a simple detector simulation, modified for the use of 1 ns-timing information. We accept photons with a rapidity $|\eta| \leq 2.1$ and a transverse energy $E_T \geq 12$ GeV according to the CDF/EMTiming fiducial region and trigger [1,2]. We first look at the efficiency of the timing system as a function of neutralino mass and lifetime for different Δs restrictions. Then we discuss background estimations and find the sensitivity for both the single and diphoton analysis.

Figure 2 shows the efficiency versus neutralino lifetime for a mass of 110 GeV$/c^2$, above the current LEP limits [13], for events with photons from neutralinos remaining in the detector and events with photons having a $\Delta s \geq 5.0$ ns. At low lifetimes, the probability that the neutralino stays in the detector is large enough that the diphoton final state dominates. At a lifetime of about 3 ns, independent of the Δs cut, single photon events become dominant. At high lifetimes the efficiency decreases rapidly for both analyses as most of the neutralinos leave the detector. Hence, in order to have sensitivity in as much lifetime range as possible, we consider both $\gamma + \not{E}_T$ and $\gamma\gamma + \not{E}_T$ analyses.

In contrast the timing efficiency is essentially constant as a function of neutralino mass at a fixed lifetime. Figure 3 shows the efficiencies at $\tau_{\tilde{\chi}} = 10$ ns, where single photon events dominate. The slight variations in the efficiency originate in the production mechanism, specifically the neutralino momentum distribution. See Appendix B for details.

TABLE I. The systematic uncertainties, estimated based on Refs. [3,11], for luminosity, acceptance, and number of background events for use in all analyses in estimating cross section limits.

Factor	Systematic uncertainty
Luminosity	5%
Acceptance	10%
Number of background events	30%

B. Backgrounds and sensitivity to neutralino pair production

To estimate the sensitivity in a quasi-model-independent manner, we consider separately single photon and diphoton events and take into account the backgrounds. All presented expected cross section limits assume no signal in the data. Throughout this section we use the relative systematic uncertainties for luminosity, acceptance, and background rates given in Table I. The expected cross section limits are calculated following [19] with the number of events observed "in the data" fluctuating around an expected mean background rate according to Poisson statistics. The cross section limit is, for a certain luminosity, a function of background events and signal acceptance, where both in turn are functions of specified cuts (e.g., Δs and $\not{E}_T$ cuts in the $\gamma\gamma + \not{E}_T$ case). After varying the cuts we find a signal acceptance and number of background

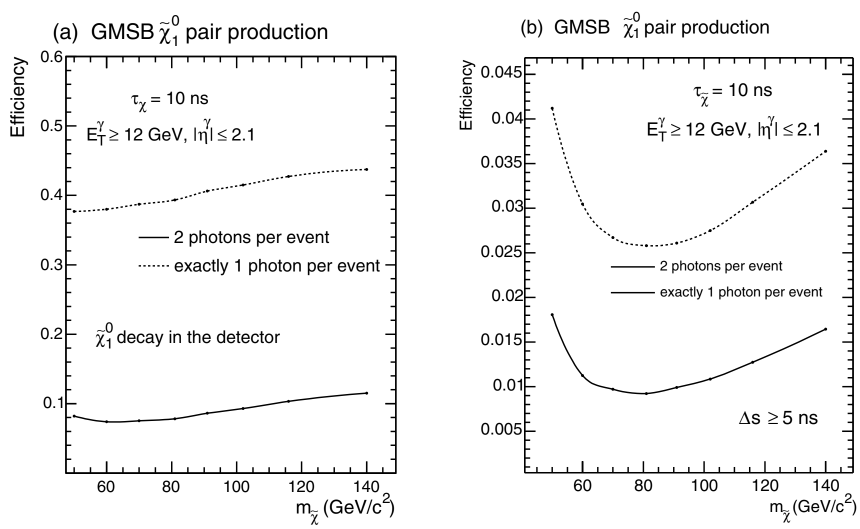

FIG. 3. The efficiency as a function of the neutralino mass at a lifetime $\tau_{\tilde{\chi}} = 10$ ns for single and diphoton events for which the neutralino decays in the detector and for $\Delta s \geq 5.0$ ns. The ratio of single to diphoton events is roughly independent of the neutralino mass and constant as a function of Δs. One can see a soft dip in the efficiency curve in a mass range of 40–80 GeV$/c^2$. This effect is production dependent and due to a change in the p_T distribution of the neutralinos (for more details, see Appendix B).

TABLE II. The background and baseline selection criteria used for the $\gamma\gamma + \not{E}_T$ analysis following Refs. [3,20].

Baseline selection requirements: $E_T^{\gamma_1} > 12$ GeV, $E_T^{\gamma_2} > 12$ GeV $\lvert\eta^{\gamma_1}\rvert < 1$, $\lvert\eta^{\gamma_2}\rvert < 1$
Backgrounds: 2577 events/100 pb^{-1} from QCD $\Delta s_{12} = \Delta s^{\gamma_1} + \Delta s^{\gamma_2}$, $\overline{\Delta s_{12}} = 0.0$ ns, $\sigma_{\Delta s_{12}} = 1.41$ ns $\not{E}_T$: Rayleigh distribution (square root of the sum of two Gaussians squared) with $\sigma = 10$ GeV
Optimization: Accept events where the event has a $\not{E}_T$ greater than the optimized $\not{E}_T$ cut or whose photons have a Δs_{12} greater than the optimized Δs_{12} cut.

events that, after smearing by systematic errors, minimizes the cross section limit.

1. $\gamma\gamma + \not{E}_T$

A $\gamma\gamma + \not{E}_T$ analysis is expected to have the best sensitivity for low neutralino lifetimes. We follow the analysis in [3] which is summarized in Table II and study the final selection requirements on $\not{E}_T$ and Δs. The background for this analysis consists of QCD events with fake $\not{E}_T$ [20]. We model the $\not{E}_T$ from QCD with a resolution of 10 GeV, i.e., we assume a measurement uncertainty of the transverse energy of all particles of 10 GeV in each x and y direction, as this reproduces well the numbers in [3] and allows us to extend our search region to large values of $\not{E}_T$. Since all photons from QCD are promptly produced, we model them with $\overline{\Delta s} = 0.0$ ns and $\sigma_{\Delta s} = 1.0$ ns. We find that adding the Δs values, $\Delta s_{12} = \Delta s^{\gamma_1} + \Delta s^{\gamma_2}$, and selecting signal events with either large $\not{E}_T$ or large Δs_{12}, either of which is not SM-like, maximizes the separation of signal and background as shown in Fig. 4. The position of the cuts is optimized for each mass and lifetime by minimizing the 95% C.L. cross section limit. We find that both the Δs_{12} and $\not{E}_T$ cuts are stable at around 7 ns and 50 GeV for nonzero lifetimes. Without timing information, we find the optimal $\not{E}_T$ cut to also be around 50 GeV.

2. $\gamma + \not{E}_T + 0$ jets

From efficiency considerations and since the signal does not produce jets at the parton level, we expect a $\gamma + \not{E}_T + 0$ jets analysis to yield the best sensitivity for longer neutralino lifetimes. We follow the analysis in [10] which is summarized in Table III and study the final selection requirements on $\not{E}_T$ and Δs. The background for this analysis is dominated by QCD, $Z\gamma$, and cosmic ray sources. Since photons from cosmic ray sources hit the detector with no correlation between the arrival time and the time of collision, we expect them to be randomly distributed over time and model this with a flat random distribution in Δs. As in the previous section, the Δs of all other SM sources is dominated by the timing resolution of 1.0 ns. The $\not{E}_T$ for the backgrounds are modeled according to the shapes in [10], and extrapolated to large values using an exponential fit. The expected background and signal shapes are shown in Fig. 5. The final cuts sort out events

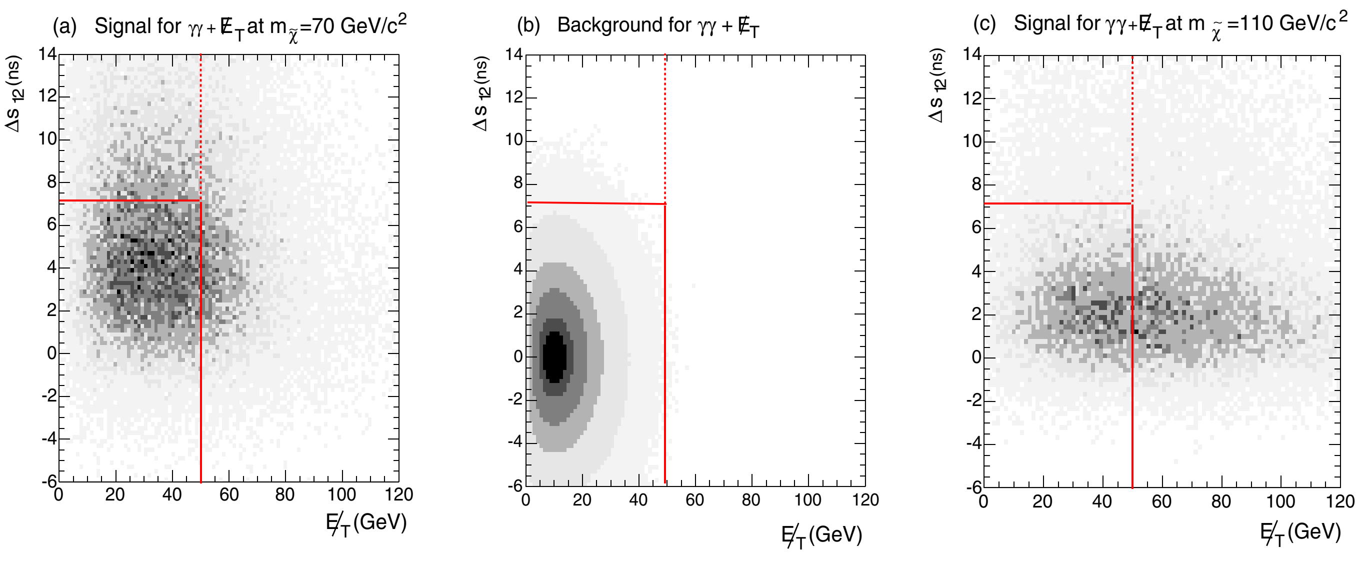

FIG. 4 (color online). The distribution of Δs_{12} and $\not{E}_T$ for signal and background in the $\gamma\gamma + \not{E}_T$ analysis (not to scale). The distributions are (a) from direct neutralino pair production, with $m_{\tilde{\chi}} = 70$ GeV$/c^2$ and $\tau_{\tilde{\chi}} = 10$ ns, (b) QCD background and (c) direct neutralino pair production, with $m_{\tilde{\chi}} = 110$ GeV$/c^2$ and $\tau_{\tilde{\chi}} = 10$ ns. The solid and dashed lines show the cuts with and without EMTiming system usage, respectively, that give the smallest 95% C.L. cross section limit. In (a) there is more additional acceptance from allowing large Δs_{12} events due to the lower mass, compared to (c), which is why the sensitivity is significantly improved with timing in this mass region (see Fig. 6).

TABLE III. The background and baseline selection criteria for the $\gamma + \not{E}_T + 0$ jets analysis following Ref. [10].

Baseline selection requirements: $E_T^\gamma > 55$ GeV $\lvert\eta^\gamma\rvert < 1.0$ $\not{E}_T > 45$ GeV No jets or additional photons with $E_T > 15$ GeV
Backgrounds: 12.6 events/100 pb^{-1} from $Z\gamma \to \nu\bar{\nu}\gamma$, $W\gamma$, $W \to e\nu$, QCD and cosmics Noncosmics: $\overline{\Delta s} = 0.0$ ns, $\sigma_{\Delta s} = 1.0$ ns Cosmics: 57% of total background, flat distribution in Δs, $\not{E}_T$ distribution according to [10] and extrapolated using an exponential function
Optimization: Accept events where the event has a $\not{E}_T$ greater than the optimized cut $\not{E}_T$ *and* the photon is in the range $\Delta s_{\rm low} \le \Delta s \le \Delta s_{\rm high}$.

with a large $\not{E}_T$ and with a photon having a Δs within a range $\Delta s_{\rm low} \le \Delta s \le \Delta s_{\rm high}$, to reject photons from SM background as well as from cosmic ray sources. We find the optimized cuts around $\Delta s_{\rm low} = -2.0$ ns, $\Delta s_{\rm high} = 2.0$ ns, and $\not{E}_T = 80$ GeV. However, $\Delta s_{\rm high}$ could vary up to 3 ns for high lifetimes, $\not{E}_T$ up to 120 GeV for higher masses. Without timing information the optimal $\not{E}_T$ cut is mostly around 100 GeV.

3. Results

Figures 6 and 7 show the expected 95% C.L. cross section upper limits vs $\tau_{\tilde{\chi}}$ for $m_{\tilde{\chi}} = 110\ \mathrm{GeV}/c^2$ and vs $m_{\tilde{\chi}}$ for $\tau_{\tilde{\chi}} = 20$ ns for both analyses for a luminosity of 2 fb^{-1}. Figure 8 shows the ratio of the lower of the two 95% C.L. cross section limits with timing system usage and without in two dimensions. In these plots we see four trends: (1) As a function of lifetime the cross section limits rise since the probability that the neutralinos decay in the detector goes down. (2) At high lifetimes the timing handle is better able to separate the signal from the backgrounds and produces better limits relative to kinematics alone. (3) As a function of mass the limits decrease as more events pass the kinematic thresholds. (4) At low masses the timing handle is better able to separate the signal from the backgrounds due to a lower $\not{E}_T$. A comparison of Figs. 4(a) and 4(c) shows how the timing and kinematic information provide complementary acceptance at different masses.

As expected, the $\gamma\gamma + \not{E}_T$ analysis yields lower cross section limits when the mass or the lifetime is low. The limit ratio is greatest in this region and occurs at a mass around 50 GeV/c^2 and a lifetime of 10–20 ns. The $\gamma + \not{E}_T + 0$ jets analysis yields lower cross section limits for the rest of the considered lifetime range and masses. Note that the course of the separation line of the analyses depends on the production momentum distribution of the neutralino.

This analysis cannot be applied to search for long-lived NLSP neutralinos in a true GMSB model with the preferred production processes, as there the neutralinos are produced as part of cascades from gaugino pairs that produce jets. Therefore, we do a separate analysis for a full GMSB production in the next section.

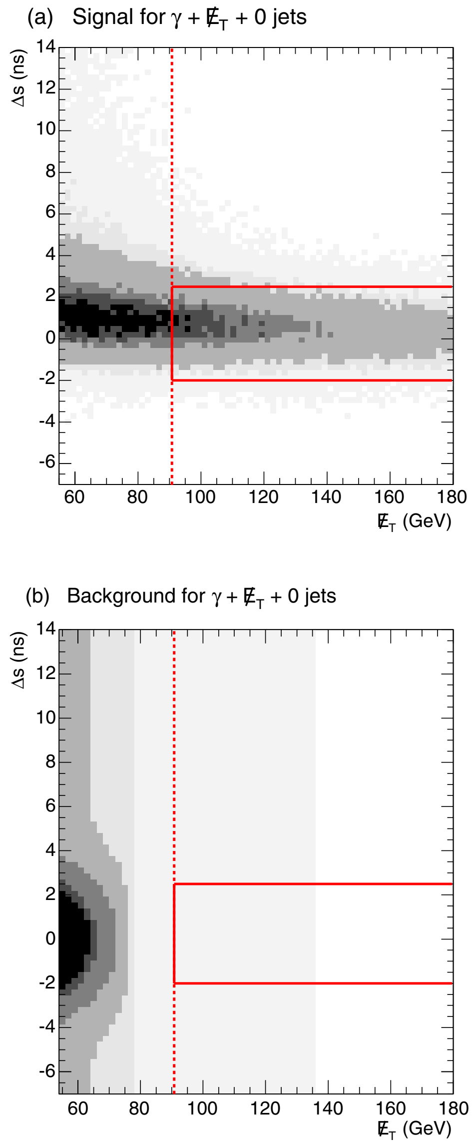

FIG. 5 (color online). The distribution of Δs vs $\not{E}_T$ for signal and background in the $\gamma + \not{E}_T + 0$ jets analysis (not to scale). The distributions are (a) from direct neutralino pair production, with $m_{\tilde{\chi}} = 110\ \mathrm{GeV}/c^2$ and $\tau_{\tilde{\chi}} = 10$ ns, and (b) from SM background. The solid and dashed lines show the cuts with and without timing system usage, respectively, that give the smallest 95% C.L. cross section limit.

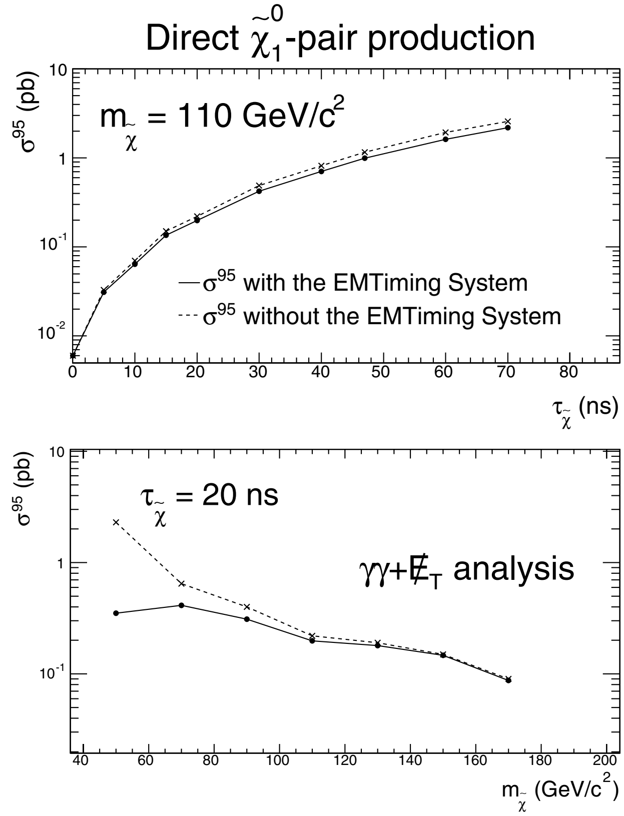

FIG. 6. The expected 95% C.L. cross section limits on direct neutralino pair production in the $\gamma\gamma + \not{E}_T$ analysis. The top plot shows the limits as a function of $\tau_{\tilde{\chi}}$ for $m_{\tilde{\chi}} = 110\ \mathrm{GeV}/c^2$. The bottom plot shows the limits as a function of $m_{\tilde{\chi}}$ for $\tau_{\tilde{\chi}} = 20$ ns for both with and without a timing system for comparison. The luminosity is 2 fb^{-1}. As expected at $\tau_{\tilde{\chi}} = 0$ ns, the cross sections merge as the timing system has no effect. For higher $\tau_{\tilde{\chi}}$ the sensitivity goes down as more photons leave the detector, but the difference of the limits increases as Δs gets larger for the signal and timing becomes more helpful. The limits get better as the mass goes up since more of the events pass the kinematic requirements; however, the timing system only provides real additional sensitivity at the lowest masses where the neutralino momentum distribution is softer.

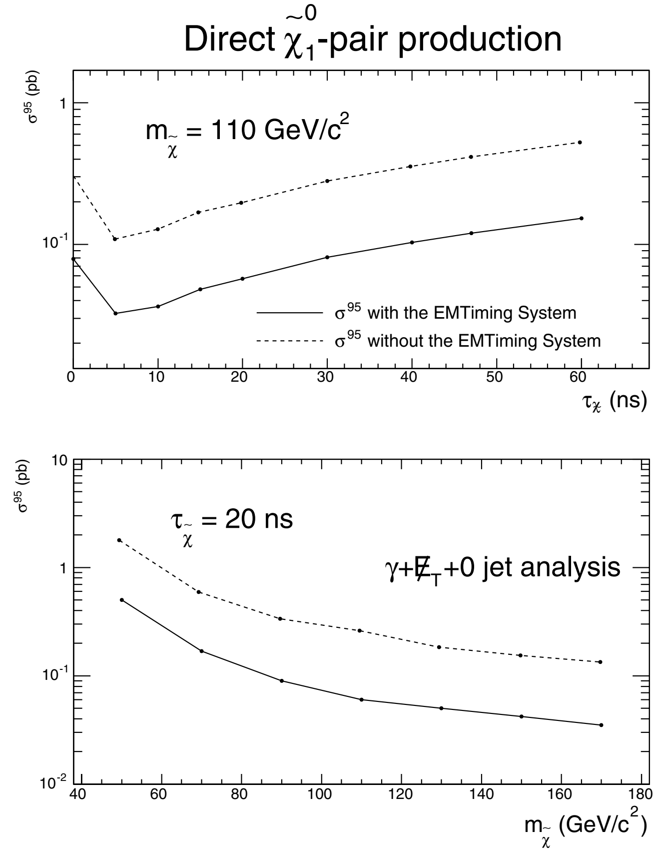

FIG. 7. The expected 95% C.L. cross section limits on direct neutralino pair production in the $\gamma + \not{E}_T + 0$ jets analysis. The top plot shows the limits as a function of $\tau_{\tilde{\chi}}$ for $m_{\tilde{\chi}} = 110\ \mathrm{GeV}/c^2$. The bottom plot shows the limits as a function of $m_{\tilde{\chi}}$ for $\tau_{\tilde{\chi}} = 20$ ns for both with and without timing. The luminosity is 2 fb^{-1}. As in Fig. 6, for higher $\tau_{\tilde{\chi}}$ the sensitivity goes down as more photons leave the detector, but the difference of the limits increases as Δs gets larger for the signal and timing becomes more helpful. The curves do not merge at 0 ns lifetime since cosmic ray backgrounds always contribute at high Δs and the timing system always has some effect on the cross section limit. The rise from 10 to 0 ns originates in an increasing probability towards zero lifetime for two photons to remain in the detector, yielding lower efficiency for a single photon analysis. The limits get better as the mass goes up since more of the events pass the kinematic requirements.

III. SENSITIVITY TO GMSB MODELS

We next consider the sensitivity to full GMSB production where we allow all processes to contribute to the final state according to their predicted cross sections. We use the same simulation tools as in Sec. II A, with the GMSB parameters chosen according to the Snowmass Slope guidelines [15] in the range where the neutralino is the NLSP. Again we consider a single photon and a diphoton analysis. The $\gamma\gamma + \not{E}_T$ analysis methodology is identical to the case of neutralino pair production. The single photon analysis must be modified to allow jets as here the neutralinos are part of cascades from gauginos that produce additional particles which, in general, could be identified as jets. We thus use a $\gamma + \not{E}_T$ + jets analysis. A study of how the results change as a function of both cosmic ray background contamination and the timing resolution is presented in Sec. III C.

A. $\gamma + \not{E}_T$ + jets

A $\gamma + \not{E}_T$ + jets analysis should be most sensitive to neutralinos with long lifetime which are produced in association with other particles in the final state such as from gaugino pair production and decay. We follow the analysis

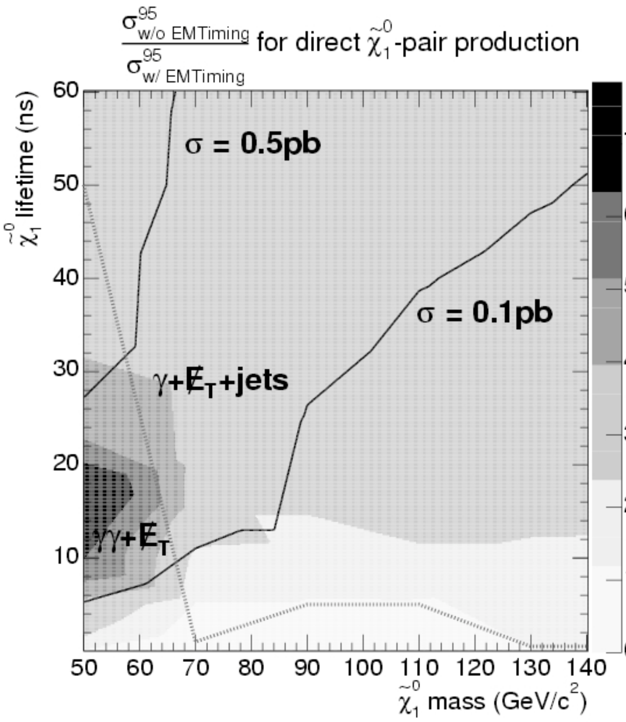

FIG. 8. This plot combines the $\gamma\gamma + \not{E}_T$ and $\gamma + \not{E}_T + 0$ jets analysis results for neutralino pair production for 2 fb^{-1} of data and is a two-dimensional visualization of Figs. 6 and 7. The contours of constant cross section limit are shown as the solid lines, and the separation line between the regions where the two different analyses provide the best sensitivity is given by the dotted line. The $\gamma + \not{E}_T + 0$ jets analysis shows better cross section limits than a $\gamma\gamma + \not{E}_T$ analysis in the mass and lifetime range above the dashed line. The shaded regions delineate the contours of the ratio of the 95% C.L. cross section limits between with and without timing information. The ratio is greatest for a low neutralino mass and a lifetime of 10–20 ns, and lowest for a high mass and low lifetime.

in [11], which is summarized in Table IV, and study the final selection requirements on $\not{E}_T$ and Δs. The backgrounds are dominated by QCD and W + jets [21]. The expected $\not{E}_T$ of the background is modeled according to Ref. [11]. Since the backgrounds are from SM, we take $\overline{\Delta s} = 0.0$ ns and $\sigma_{\Delta s} = 1.0$ ns. The signal and background shapes are shown in Fig. 9. We find that the optimal final selection requirements accept events with either large $\not{E}_T$ or large Δs. For without-timing usage, we find the optimized $\not{E}_T$ cut to be around 50 GeV for masses around 70 GeV$/c^2$, varying up to 110 GeV for masses around 150 GeV$/c^2$. For with-timing usage, we find only a Δs cut around 4 ns which is stable for all masses and lifetimes, and no $\not{E}_T$ cut other than the baseline $\not{E}_T > 25$ GeV (except for $\tau_{\tilde{\chi}} = 0$ ns where the diphoton case has the best sensitivity). While it is outside of our ability to predict, one might find further optimization is possible by further lowering the baseline $\not{E}_T$ sample requirements.

TABLE IV. The background and baseline selection criteria used for the $\gamma + \not{E}_T$ + jets analysis following Refs. [11,21].

Baseline selection requirements:
$E_T^\gamma > 20$ GeV
$\lvert\eta^\gamma\rvert < 1.1$ or $1.5 < \lvert\eta^\gamma\rvert < 2.0$
$\not{E}_T > 25$ GeV
≥ 2 jets with $E_T^{\text{jet}} > 20$ GeV and $\lvert\eta^{\text{jet}}\rvert < 2.0$
Backgrounds:
320 events/100 pb^{-1} from QCD and W + jets
$\overline{\Delta s} = 0.0$ ns, $\sigma_{\Delta s} = 1.0$ ns
$\not{E}_T$ distribution from [11], extrapolated to large $\not{E}_T$
Optimization:
Accept events where the event has a $\not{E}_T$ greater than the optimized $\not{E}_T$ cut or whose photon has a Δs greater than the optimized Δs cut.

B. Results

Figures 10 and 11 show the expected 95% C.L. cross section upper limits vs $\tau_{\tilde{\chi}}$ for $m_{\tilde{\chi}} = 110$ GeV$/c^2$ and vs $m_{\tilde{\chi}}$ for $\tau_{\tilde{\chi}} = 20$ ns for both analyses for a luminosity of 2 fb^{-1}. Figure 12 shows the ratio of the lowest 95% C.L. cross section limits with timing system usage and without in two dimensions. We see the same general trends as in neutralino pair production as the signal shapes are similar in both analyses. Table V shows more details on the analyses for selected points in the $m_{\tilde{\chi}}$-$\tau_{\tilde{\chi}}$ plane.

A comparison of the cross section limits with the production cross sections in the GMSB model at a luminosity of 2 fb^{-1} gives the mass vs lifetime exclusion regions shown in Fig. 13. As expected, timing has the biggest effect at low masses and high lifetimes. We have also indicated the exclusion regions from ALEPH at LEP II from both direct and indirect searches [13]. ALEPH effectively excludes all neutralino masses under 80 GeV$/c^2$ up to high lifetimes, with a small extension to 100 GeV$/c^2$ for lifetimes below 20 ns. For 2 fb^{-1}, in Run II, the Tevatron should significantly extend the sensitivity at large mass and lifetimes. The mass exclusion limit at 168 GeV for $\tau_{\tilde{\chi}} = 0$ ns is comparable to the limit presented in the D0 study of displaced photons in Ref. [22], but for large lifetimes this result significantly extends the reach. Since in most cosmological scenarios the relic density of the gravitino will overclose the universe if it has a mass of $\geq$ few keV$/c^2$ [14], we show the 1 keV$/c^2$ line as an indicator for this theoretically preferred region. While variations from the chosen GMSB model line have not been further examined, the highest gravitino mass we can exclude is $\sim$1.7 keV$/c^2$ at $m_{\tilde{\chi}} \approx 130$ GeV$/c^2$ and $\tau_{\tilde{\chi}} \approx 60$ ns.

C. Factors that might change the cross section limit

While we have taken the best available nominal values from the references for both the contamination of cosmic ray background events and the timing resolution in the

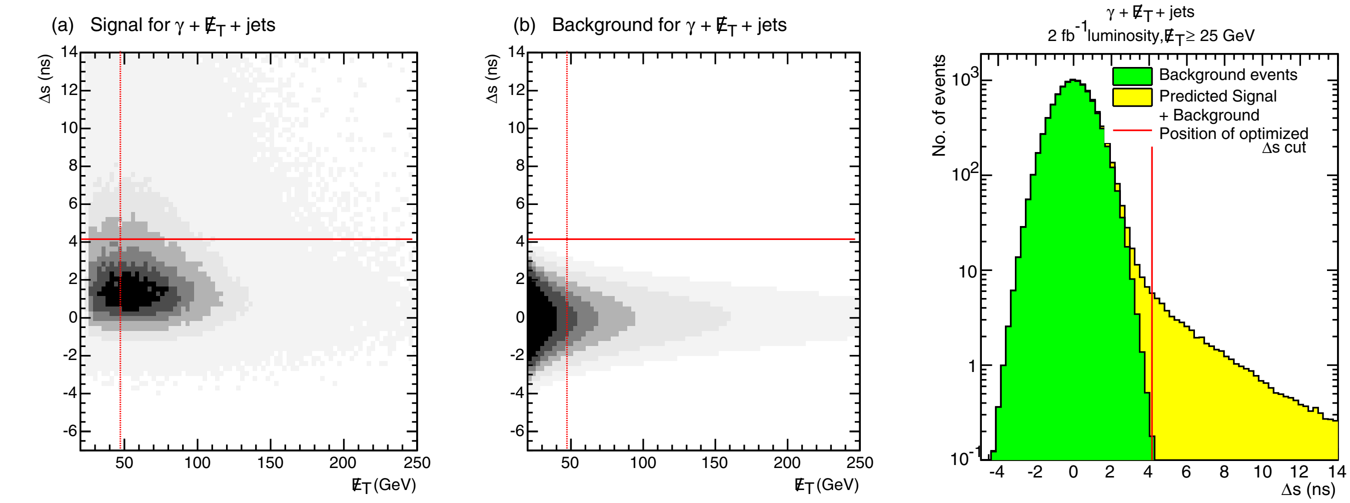

FIG. 9 (color online). The distribution of Δs vs $\not{E}_T$ for signal and background in the $\gamma + \not{E}_T +$ jets analysis (not to scale). The distributions are (a) from full GMSB production, with $m_{\tilde{\chi}} = 110\ \mathrm{GeV}/c^2$ and $\tau_{\tilde{\chi}} = 10$ ns, (b) from SM background and (c) from both as a function of Δs after the baseline $\not{E}_T$ cut of 25 GeV. The solid and dashed lines show the cuts with and without timing system usage, respectively, that give the smallest 95% C.L. cross section limit.

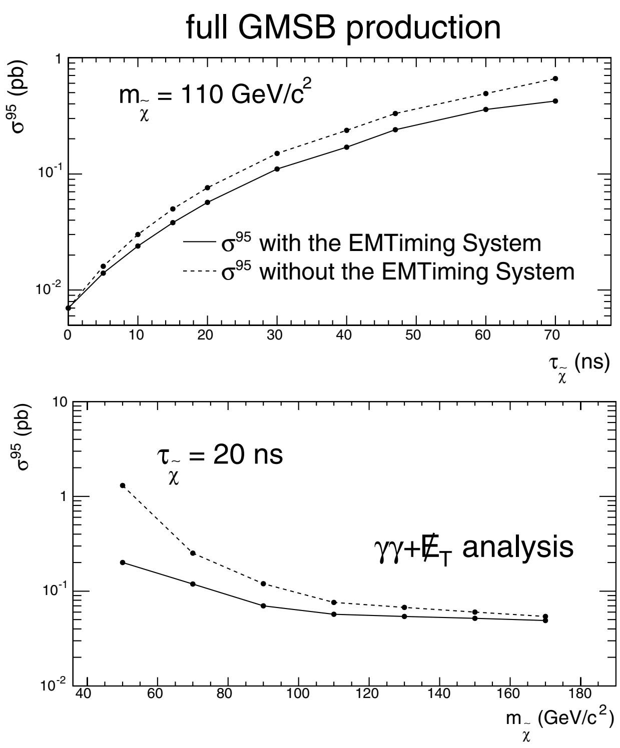

FIG. 10. The expected 95% C.L. cross section limits on full GMSB production in a $\gamma\gamma + \not{E}_T$ analysis. The top plot shows the limits as a function of $\tau_{\tilde{\chi}}$ for $m_{\tilde{\chi}} = 110\ \mathrm{GeV}/c^2$. The bottom plot shows the limits as a function of $m_{\tilde{\chi}}$ for $\tau_{\tilde{\chi}} = 20$ ns for both with and without a timing system. The luminosity is 2 fb^{-1}. The results are similar to those in Fig. 6.

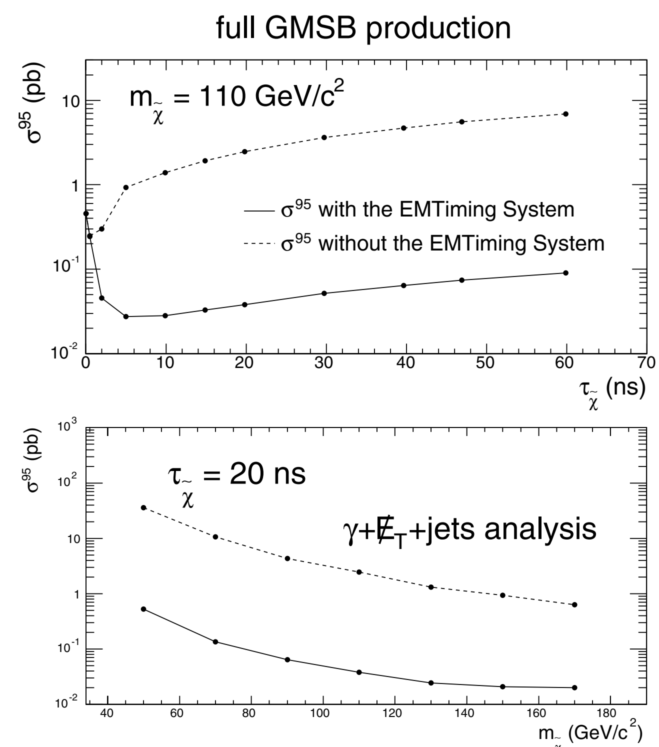

FIG. 11. The expected 95% C.L. cross section limits on full GMSB production in a $\gamma + \not{E}_T +$ jets analysis. The top plot shows the limits as a function of $\tau_{\tilde{\chi}}$ for $m_{\tilde{\chi}} = 110\ \mathrm{GeV}/c^2$ and the bottom plot as a function of $m_{\tilde{\chi}}$ for $\tau_{\tilde{\chi}} = 20$ ns for both with and without timing. The luminosity is 2 fb^{-1}. For all but the lowest lifetimes, the timing information significantly improves the cross section limits. Note that here the cross sections merge at zero lifetime since we have neglected cosmics in this analysis following [11,21].

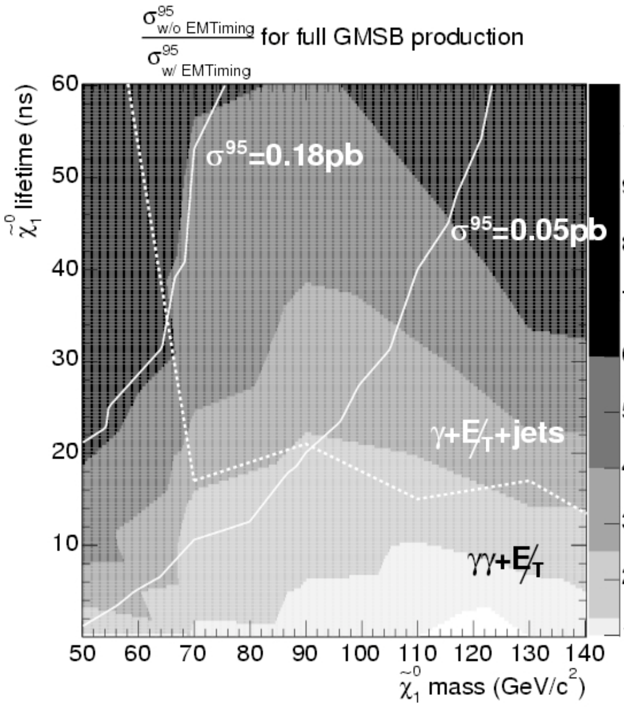

FIG. 12. This plot combines the $\gamma\gamma + \not{E}_T$ and $\gamma + \not{E}_T$ + jets analysis results for a full GMSB model simulation for 2 fb^{-1} and is a two-dimensional visualization of Figs. 10 and 11. The contours of constant cross section limit are shown as the solid lines. The separation line between the regions where the two different analyses provide the best sensitivity is given by the dotted line. The $\gamma + \not{E}_T$ + jets analysis shows better cross section limits than a $\gamma\gamma + \not{E}_T$ analysis in the mass and lifetime range above the dashed line. The shaded regions delineate the contours of constant ratio of the 95% C.L. cross section limits between with and without timing information. The EMTiming system has its most effective region at high lifetime while the kinematics give the best separation at high masses.

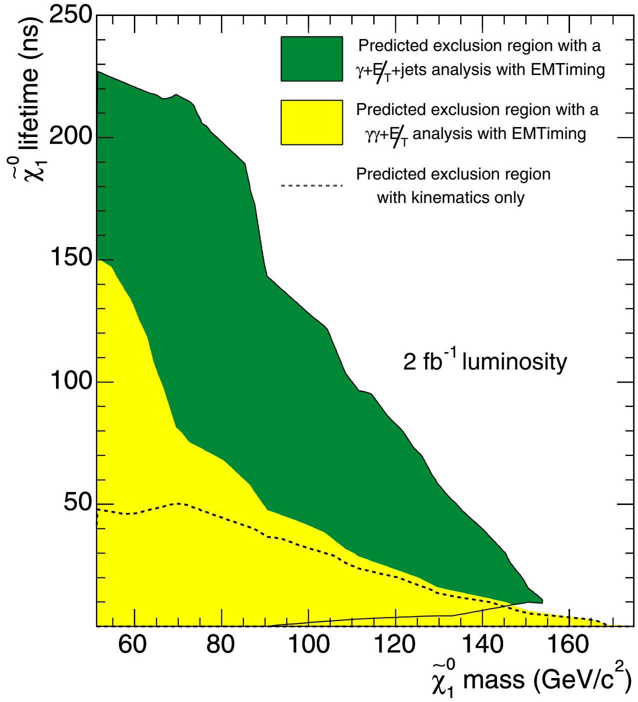

FIG. 13 (color online). The expected 95% C.L. exclusion regions as a function of neutralino lifetime and mass for full GMSB production at 2 fb^{-1} luminosity for the $\gamma\gamma + \not{E}_T$ and the $\gamma + \not{E}_T$ + jets analysis separately. The region below the dashed line is the expected exclusion region from kinematics alone, i.e., where no timing information is used.

$\gamma\gamma + \not{E}_T$ and $\gamma + \not{E}_T$ + jets analyses, the limits are sensitive to variations of these values. For simplicity, rather than include them as a systematic error we estimate the variation of the results for these effects on the cross section limits for a neutralino mass of 110 GeV$/c^2$ and a lifetime of 40 ns (beyond the ALEPH exclusion region). Figure 15 shows the cross section limit as a function of the fraction of events which are from cosmics in the background sample. Using the same analysis style as in the $\gamma + \not{E}_T$ + 0 jets case, we find cuts around $\Delta s_{\mathrm{low}} = 3.0$ ns and $\not{E}_T = 55$ GeV, with Δs_{high} varying from infinity down to 7 ns with a rising fraction of cosmics. The limits rise approximately linearly as a function of the fraction of events which are from cosmics. An upper bound on the fraction of cosmics of 10% would reduce the limits by about a factor of 4; a more reasonable estimate is probably 1%–5% which would raise the cross section limits by a factor of 2–3.

TABLE V. Selected points from both GMSB analyses after the optimized cuts. Shown are the number of expected signal events (N_S) and background events (N_B), the LO production cross section (σ_{prod}), and the expected cross section limit (σ^{95}). For the uncertainties on the number of signal and background events, see Table I.

			Optimized cuts					
$m_{\tilde{\chi}}$ (GeV)	$\tau_{\tilde{\chi}}$ (ns)	Analysis	Δs (ns)	$\not{E}_T$ (GeV)	N_S	N_B	σ_{prod} (fb)	σ^{95} (fb)
90	20	$\gamma\gamma + \not{E}_T$	6.7	52.7	16.6	0.06	320	66
130	10	$\gamma\gamma + \not{E}_T$	6.7	52.7	5.6	0.06	38	23
110	60	$\gamma + \not{E}_T$ + jets	4.2	25	5.5	0.05	108	70
70	190	$\gamma + \not{E}_T$ + jets	4.2	25	4.0	0.17	1101	955
110	125	$\gamma + \not{E}_T$ + jets	4.2	25	2.7	0.17	108	141

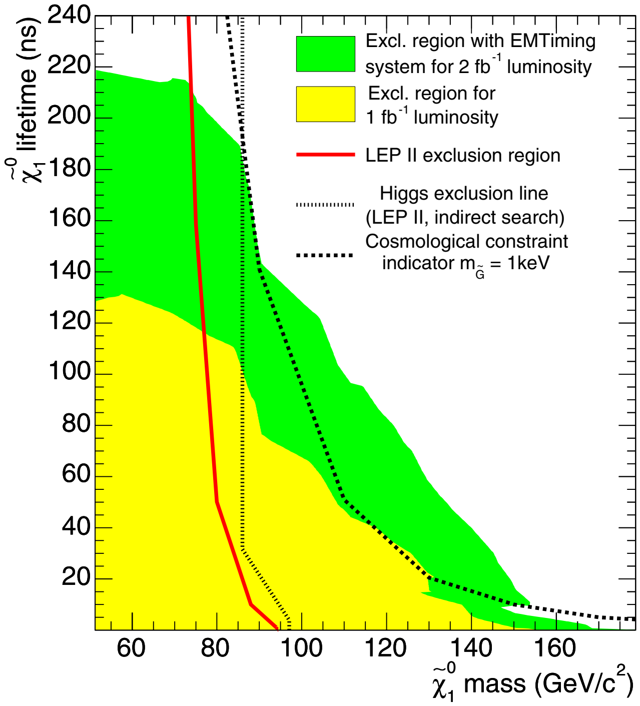

FIG. 14 (color online). The expected 95% C.L. exclusion regions as a function of neutralino lifetime and mass for full GMSB production from the overlap of both the $\gamma\gamma + \not{E}_T$ and the $\gamma + \not{E}_T$ + jets analysis for 1 fb^{-1} and 2 fb^{-1} luminosity. The result is compared to the direct and indirect search limits from ALEPH at LEP II [13,25] and the $m_{\tilde{G}} = 1$ keV$/c^2$ line as an indicator for the theoretically favored region from cosmological considerations [14]. The Tevatron in Run II should be able to significantly extend the LEP II limits and provide sensitivity in the favored region for all masses below about 150 GeV$/c^2$ for the considered GMSB model line.

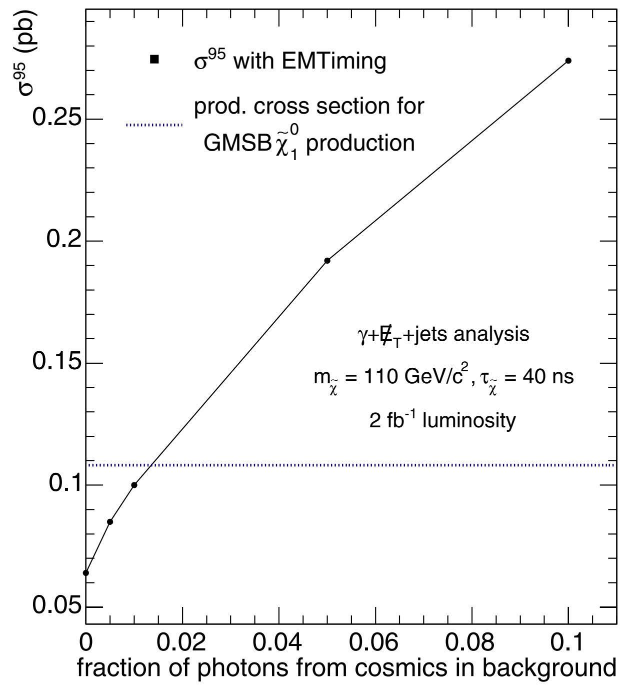

FIG. 15 (color online). The expected 95% C.L. cross section limit for full GMSB production at $m_{\tilde{\chi}} = 110$ GeV$/c^2$ and $\tau_{\tilde{\chi}} = 40$ ns as a function of the fraction of the background from cosmic ray sources for a $\gamma + \not{E}_T$ + jets analysis. The cross section limits rise approximately linearly as a function of the fraction and 10% provides an outer bound on this fraction. A more reasonable fraction is probably 1%–5% which roughly doubles the cross section limit value.

The limits are potentially more sensitive to the resolution. Figure 16 shows how the limits change as a function of the timing resolution for the same mass and lifetime, in the $\gamma + \not{E}_T$ + jets analysis. The limits are fairly stable (with the same factor of 2) for resolutions within 20% of the nominal 1 ns resolution. Note that the position of the "turn-on," where the limit changes drastically, depends on neutralino mass/lifetime. There is good reason to believe that the resolution will be better than advertised [7].

IV. CONCLUSION

We have studied the prospects of using timing information to directly search for neutral, long-lived particles which decay to photons, as one can find in SUSY models. With the EMTiming system at CDF as an example, we find that a combination of timing and kinematic requirements provides excellent rejection against SM backgrounds in complementary fashion. As the mass increases, the kinematics are more important and the sensitivity gets better. For a given mass, as the lifetime increases, more of the neutralinos leave the detector and the overall sensitivity goes down. However, timing provides additional rejection power and allows for significant exclusions even at large lifetimes and improves the cross section limits by a factor of 5–10 at lifetimes around 50 ns. While the region where timing produces the most additional rejection is already excluded by ALEPH at LEP II, the additional handle it provides should allow the Tevatron in Run II to produce the world's most stringent limits at masses above 80 GeV$/c^2$ at high lifetimes. These exclusions have the potential to come close to cosmological constraints for GMSB models.

ACKNOWLEDGMENTS

The authors would especially like to thank T. Kamon for his early contributions to the genesis of the idea of using the EMTiming system at CDF to search for GMSB SUSY; it was his preliminary feasibility study which showed that the analysis might be possible. We would also like to thank R. Arnowitt, R. Culbertson, B. Dutta, A. Garcia-Bellido, M. Goncharov, V. Khotilovich, V. Krutelyov, S. W. Lee, P. McIntyre, and S. Mrenna for help and useful discussions.

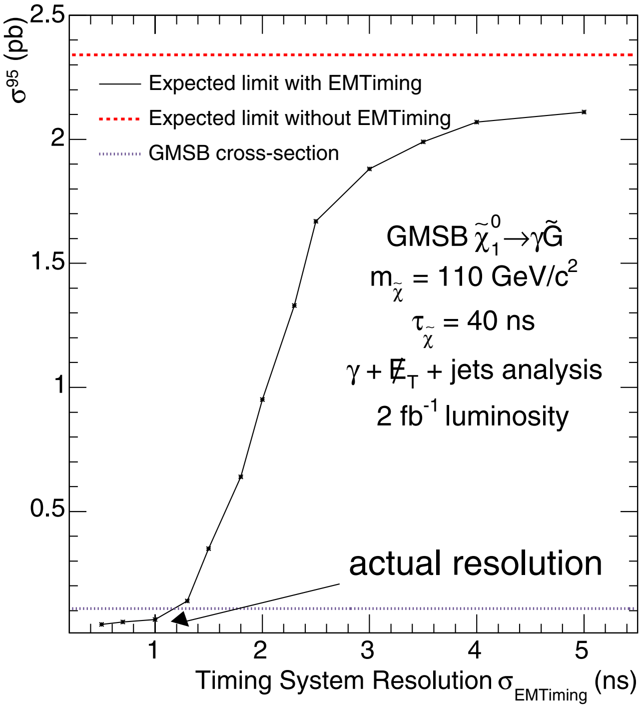

FIG. 16 (color online). The 95% C.L. cross section limits vs timing system resolution for $m_{\tilde{\chi}} = 110\ \mathrm{GeV}/c^2$ and $\tau_{\tilde{\chi}} = 40$ ns at 2 fb^{-1} luminosity in the $\gamma + \not{E}_T$ + jets analysis. As expected, for large resolution the cross section with EMTiming approaches the cross section without EMTiming. A system resolution of 1.0 ns improves the cross section limit by a factor of about 20, but this varies as a function of mass, lifetime as well as on the analysis. It is reasonable to assume that the resolution will be within 20% of the nominal 1.0 ns presented here.

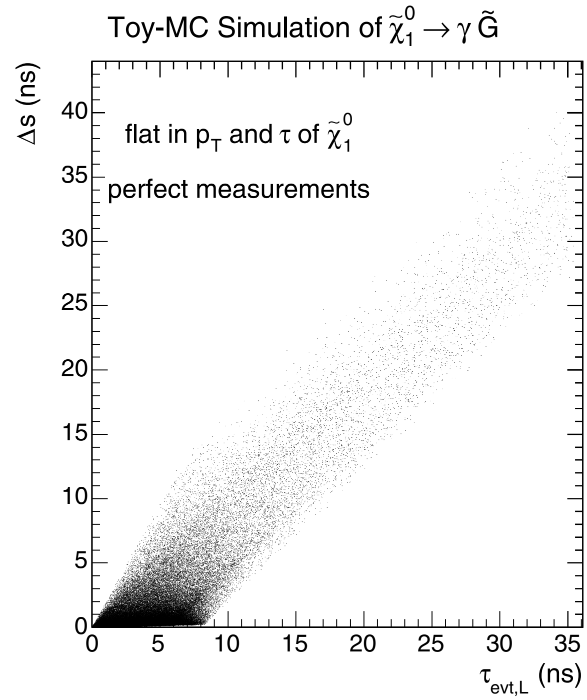

FIG. 17. The Δs distribution as a function of the event lifetime in the neutralino lab frame for a toy Monte Carlo simulation. In general, Δs is proportional to $\tau_{\mathrm{evt,L}}$. At large $\tau_{\mathrm{evt,L}}$ most of the neutralinos leave the detector and are not shown here. The spread perpendicular to $\Delta s \sim \tau_{\mathrm{evt,L}}$ originates in variations of the neutralino velocity as well as in variations in the travel time of the photon due to detector geometry. Essentially, photons with large Δs require a neutralino with a long lifetime.

We thank Fermilab and the CAF system administrators for providing additional computing power. This research was generously supported using funding from the College of Science and the Department of Physics at Texas A&M University.

APPENDIX A: KINEMATIC PROPERTIES OF EVENTS WITH LONG-LIVED PARTICLES WHICH DECAY TO PHOTONS

While the final sensitivity studies use both a full physics generation and a detector simulation of the geometry and timing resolution, it is useful to show the kinematic properties of events which yield large Δs measurements using a "toy Monte Carlo" with perfect resolution. Neutral particles, which we will refer to as neutralinos, are simulated independent of their mass as emanating isotropically from the center of the detector and emit a photon isotropically after a lifetime $\tau_{\tilde{\chi}}$ in their rest frame. Neutralinos are simulated with a flat velocity and lifetime distribution; i.e., independently any lifetime and velocity have equal probability.

Figure 17 shows the measured Δs versus the event lifetime of the $\tilde{\chi}_1^0$ in the lab frame, $\tau_{\mathrm{evt,L}}$. For $\Delta s \gtrsim 10$ ns there is a roughly linear relation between Δs and $\tau_{\mathrm{evt,L}}$. For a fixed $\tau_{\mathrm{evt,L}}$ the maximum Δs (upper bound) occurs when the neutralino travels to the farthest corner of the detector and then emits a photon backward to the opposite corner. Analogously, we get a minimum Δs (lower bound) if the neutralino travels with high velocity to the nearest part of the detector and emits a photon forward. The latter would look like a usual prompt photon event except for the difference in velocity between the neutralino and the photon. If the event lifetime is greater than the maximum time, a prompt photon would need to travel to the detector; then Δs is restricted from below and $\Delta s > 0$ ns (given that the neutralino decays inside the detector). Thus, the spread mainly comes from detector geometry but with the neutralino velocity also contributing to the width.

Figure 18 shows Δs versus the neutralino boost for the lifetime slice 8.5 ns $\leq \tau_{\mathrm{evt,L}} \leq 9.0$ ns. A low boost (between 1.0 and 1.5) allows large Δs since neutralinos can have a larger lifetime without leaving the detector. Neutralinos with high boost are more likely to leave the detector, and even if they do not and their photon is detected, it has low Δs (0 ns $\lesssim \Delta s \lesssim 2$ ns). Thus, photons

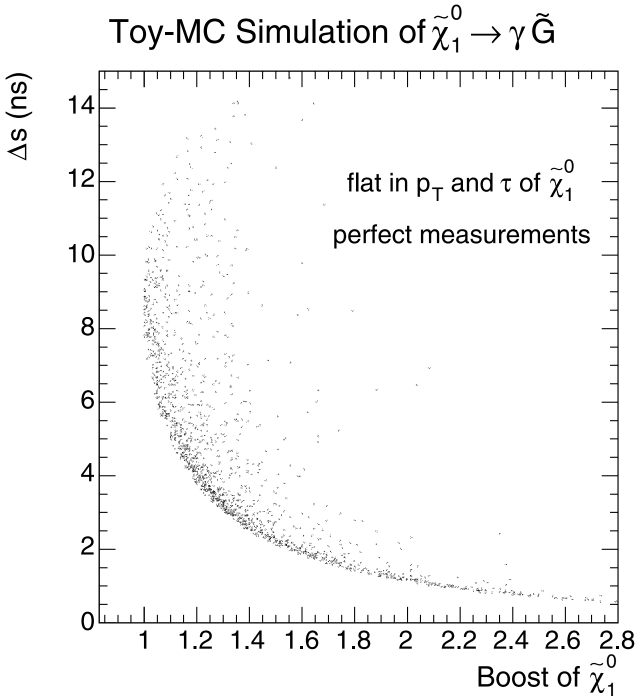

FIG. 18. The Δs distribution as a function of the boost of the neutralino for a lifetime "slice" of 8.5 ns $\leq \tau_{\mathrm{evt,L}} \leq$ 9.0 ns. In the region $1.0 <$ boost < 1.5 neutralinos remain in the detector and can produce a large Δs. Neutralinos with high boost, that is high p_T, are more likely to leave the detector or, if they do not, produce low Δs. Thus, events with the largest Δs are produced by neutralinos with large lifetimes and low boosts.

with large Δs are produced by neutralinos with long lifetimes and low boost.

Next we consider the efficiency for neutralinos to remain in the detector and/or produce a photon with large Δs. Figure 19 shows the efficiency, the fraction of all generated events that produce photons which pass a given Δs restriction, as a function of the event lifetime, τ_{evt}, for neutralinos which decay in the detector ($\Delta s \geq 0.0$ ns), $\Delta s \geq 3.0$ ns and 5.0 ns for the same production distribution. While these results change for a more realistic p_T spectrum, the qualitative features remain the same and are instructive. In the limit of $\tau_{\mathrm{evt}} = 0$ ns and $\Delta s \geq 0.0$ ns, the efficiency is 100% and the efficiency decreases with higher event lifetime since the neutralinos are more likely to leave the detector. When one applies a Δs requirement, however, there is no efficiency for events that contain neutralinos with a low event lifetime ($\tau_{\mathrm{evt}} \lesssim 2$ ns). For any $\Delta s > 0$ requirement the efficiency goes to 0% at $\tau_{\mathrm{evt}} = 0$ ns, since all photons would have $\Delta s = 0$. A higher Δs cut gradually suppresses events with a neutralino lifetime of about $\tau_{\mathrm{evt}} \lesssim 2 \cdot \Delta s$, whereas it does not suppress any events with a high lifetime. So, if an event contains a neutralino with a long lifetime, and which decays in the detector, the decay photon always has high Δs.

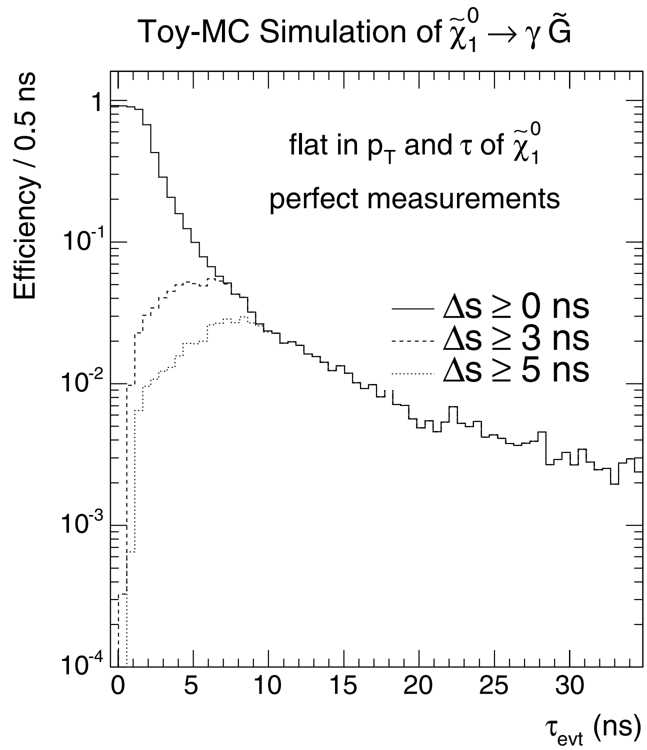

FIG. 19. The efficiency as a function of the event lifetime, τ_{evt}, of the neutralino. We distinguish between events in which the neutralino remains in the detector, and events with photons of medium and large Δs. The efficiency is 100% for prompt decays (a small difference shows up as a binning effect) for a photon to be identified, but only a very small efficiency for events with low τ_{evt} at large Δs. At large τ_{evt}, only few events stay in the detector; however, if a neutralino is long-lived and stays in the detector, it has large Δs. We note that the true efficiency shape depends on the production mechanism, i.e., the neutralino p_T distribution.

APPENDIX B: COMMENTS ON THE NEUTRALINO MASS DEPENDENCY OF THE EFFICIENCY

The "dip" in the efficiency as a function of neutralino mass shown in Fig. 3 can be explained by the neutralino pair production mechanism. If the decay length is greater than the distance to the detector wall, the neutralino will leave. Since this is proportional to the ratio of the neutralino's transverse momentum to its mass, $\frac{p_T}{m}$ (at constant lifetime), the dip occurs from a change in the shape of the $\frac{p_T}{m}$ distribution of the neutralinos as shown in Fig. 20. For a mass of 80 GeV$/c^2$ the maximum moves towards higher $\frac{p_T}{m}$ and the distribution broadens compared to 40 GeV$/c^2$, yielding a greater fraction of high-p_T neutralinos and, hence, a loss in efficiency. As the mass gets higher the maximum remains the same and the distribution narrows, which in turn leads to a gain in efficiency. Thus, the efficiency is essentially independent of the neutralino mass, with slight variations originating from the produc-

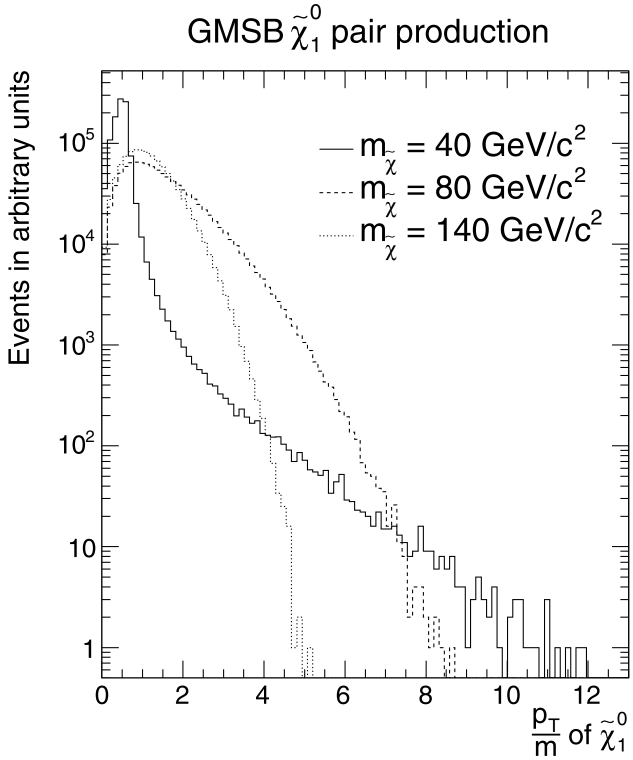

FIG. 20. The neutralino $\frac{p_T}{m}$ distribution for masses 40, 80, and 140 GeV$/c^2$ for neutralino pair production. For a mass of 80 GeV$/c^2$, the maximum moves towards higher $\frac{p_T}{m}$ and the distribution broadens compared to 40 GeV$/c^2$, yielding a greater fraction of high p_T neutralinos which either leave the detector or produce low Δs photons, and thus a loss in efficiency. For higher masses the maximum remains constant and the distribution narrows so the efficiency rises.

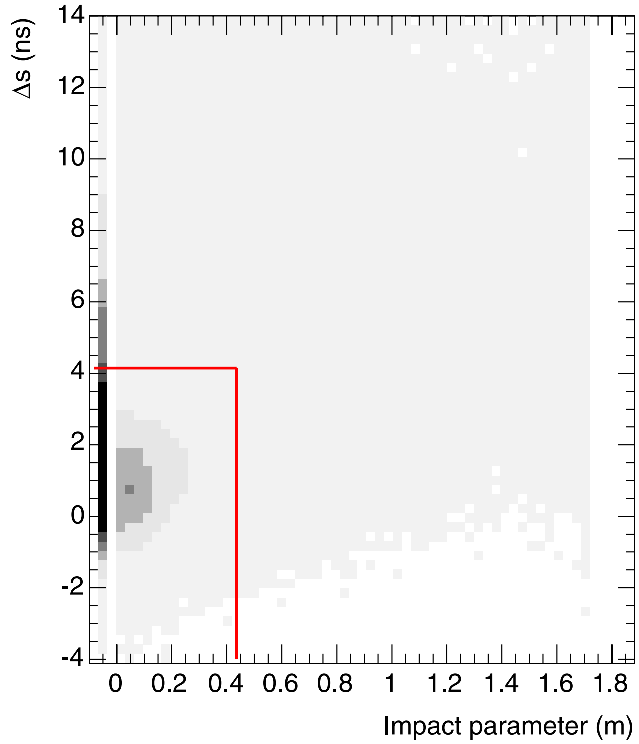

FIG. 21 (color online). The relationship between Δs and the impact parameter, b, of a photon from $\tilde{\chi}_1^0 \rightarrow \gamma \tilde{G}$ decays in a GMSB model with $m_{\tilde{\chi}} = 110$ GeV$/c^2$ and $\tau_{\tilde{\chi}} = 10$ ns. The solid lines show the selection requirements that give us the smallest 95% C.L. cross section limit in a $\gamma + \not{E}_T +$ jets analysis. The photons without impact parameter measurement are assigned a $b < 0$ m. Because of the low cut on the impact parameter, there are about as many events in the low-Δs high-b as in the high-Δs low-b region. This leads to a similar efficiency for a pure b cut compared to a pure Δs cut. The combined restriction leads to improved signal sensitivity.

tion mechanism, specifically the neutralino momentum distribution.

APPENDIX C: PHOTON POINTING

As shown in Fig. 14, ALEPH has already excluded the low neutralino mass region using a photon pointing method [13]. In this section, we compare the EMTiming system to a potential photon pointing ability at CDF. A nonzero lifetime can result in a macroscopic decay length and impact parameter, where the impact parameter of the photon is basically the closest distance of the trajectory to the collision point. While CDF has never used its calorimeter for a pointing measurement, it is possible to use the central EM strip/wire gas chamber (CES) and the central preradiator gas chamber (CPR) at CDF to measure two points along the photon trajectories that determine the direction of the photon, and trace it back to yield the impact parameter [23]. Since the CPR has no z-measurement ability, this allows only a measurement of the radial component of the impact parameter with an estimated resolution of 10 cm (see Table VI). One of the primary reasons this has not been used is that the conversion, i.e., measurement, probability, is ∼65%, with an angular dependence obtained with

$$P_C = 1 - e^{-(7/9)(N_{\rm rad}/\sin\theta)},$$

where $N_{\rm rad} = 1.072$ is the number of radiation lengths before the CPR, and θ is the angle with respect to the beam line [24].

TABLE VI. Photon pointing parameters for the CDF detector [23]. With this combination we estimate that an impact parameter measurement may be possible with a resolution of 10 cm in the radial direction.

Measurement only in radial direction	
Radius of CES	184.15 cm
Radius of CPR	168.29 cm
$\sigma_{\rm CES}$	2 mm
$\sigma_{\rm CPR}$	5 mm
$N_{\rm rad}$	1.072 X_0

To estimate the sensitivity with a pointing method, we consider a $\gamma + \not{E}_T +$ jets analysis. Figure 21 shows the distribution of the signal events as a function of impact parameter and Δs taking into account the measurement probability. There are roughly as many events in the region of low impact parameter and high Δs as there are at high impact parameter and low Δs. Hence, either method should have roughly the same effect on the exclusion region, as confirmed by Fig. 22, which shows the expected exclusion region in the mass-lifetime plane. While timing is better than pointing by itself, if pointing turns out to be feasible, a combination of the two would further improve the sensitivity.

Considered separately, a second advantage of timing is that it "filters" manifestly long lifetime events, whereas the impact parameter allows also short lifetime-high momentum events. Another possible advantage of the combination is that, if there is an excess, we could draw more information about the individual events, for instance determine the direction of the photon. With the x-y direction of the photon momentum being fixed, e.g., by the CPR/CES measurement at CDF, we can use the timing system to measure the z component, if we assume the neutralino boost to be ~1.0 which is typically the case. Or if hypothetically the pointing would provide z and x-y components, one could possibly determine the position of the vertex and thus the decay time. However, with the current 1.0 ns resolution, the photon vertex position resolution would be roughly 50 cm.

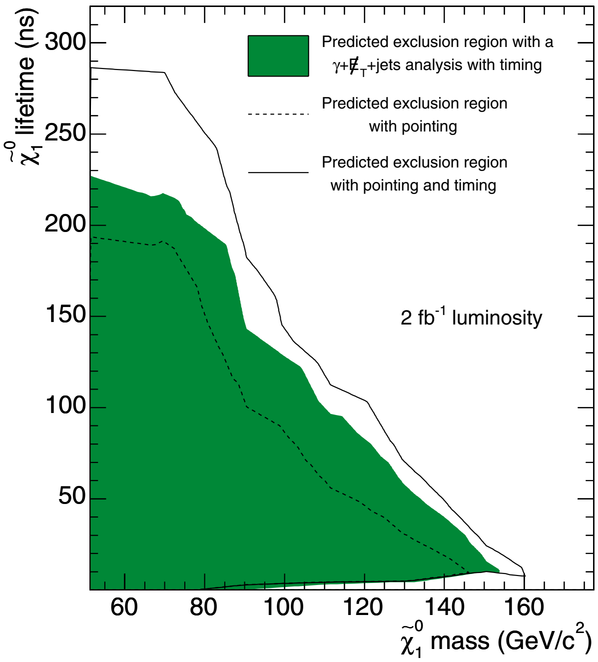

FIG. 22 (color online). A comparison of the expected exclusion regions as a function of neutralino mass and lifetime for the GMSB model at 2 fb^{-1} luminosity for a $\gamma + \not{E}_T +$ jets analysis with photon pointing and timing. While timing generally yields a higher sensitivity than pointing, both methods would, if available and combined, extend the exclusion region further than either of them alone.

[1] CDF II Collaboration, F. Abe *et al.*, FERMILAB-Pub-96/390-E.

[2] S. Kuhlmann *et al.*, Nucl. Instrum. Methods Phys. Res., Sect. A **518**, 39 (2004); CDF Collaboration, P. T. Lukens, FERMILAB-TM-2198; for more details, see http://hepr8.physics.tamu.edu/hep/emtiming/.

[3] See, for example, CDF Collaboration, F. Abe *et al.*, Phys. Rev. D **59**, 092002 (1999); Phys. Rev. Lett. **81**, 1791 (1998).

[4] Note that in principle the system can be used in conjunction with the time of flight system to search for charged particles as well. This becomes especially interesting for events in which the charged particle decays in flight and no track is reconstructed.

[5] See, for example, S. Ambrosanio, G. L. Kane, G. D. Kribs, S. P. Martin, and S. Mrenna, Phys. Rev. D **54**, 5395 (1996); C. H. Chen and J. F. Gunion, Phys. Rev. D **58**, 075005 (1998).

[6] At CDF x_f is measured by the shower-maximum detector (CES/PES) in the electromagnetic calorimeter and x_i is the collision point, measured by the silicon vertex chamber (SVX). The t_i is calculated by the central outer tracker (COT) and the time of flight (TOF) system which uses the momentum and the measured time of flight of the charged particles of the underlying event emerging from the collision point, and t_f is the time of arrival of the photon from the EMTiming system.

[7] M. Goncharov (private communication). Note that with more data the system will be better understood, possibly leading to even lower resolution.

[8] D0 Collaboration, S. Abachi *et al.*, Nucl. Instrum. Methods Phys. Res., Sect. A **338**, 185 (1994).

[9] D0 Collaboration, S. Abachi *et al.*, Phys. Rev. Lett. **78**, 2070 (1997); B. Abbott *et al.*, Phys. Rev. Lett. **80**, 442 (1998).

[10] CDF Collaboration, D. Acosta *et al.*, Phys. Rev. Lett. **89**, 281801 (2002).

[11] D0 Collaboration, B. Abbott *et al.*, Phys. Rev. Lett. **82**, 29 (1999).

[12] Note that we do not assume that any search for long-lived particles analysis without EMTiming at CDF is robust enough since there are no current collider experiments which have results without an additional handle such as photon pointing as done at LEP or D0. For a discussion of photon pointing, see, for example, ALEPH Collaboration, D. Decamp *et al.*, Nucl. Instrum. Methods Phys. Res.,

Sect. A **294**, 121 (1998); D. Cutts and G. Landsberg, hep-ph/9904396.

[13] ALEPH Collaboration, A. Heister *et al.*, Eur. Phys. J. C **25**, 339 (2002); A. Garcia-Bellido, Ph.D. thesis, Royal Holloway University of London, 2002, hep-ex/0212024.

[14] H. Pagels and J.R. Primack, Phys. Rev. Lett. **48**, 223 (1982); T. Moroi, H. Murayama, and M. Yamaguchi, Phys. Lett. B **303**, 289 (1993).

[15] We follow B.C. Allanach *et al.*, Eur. Phys. J. C **25**, 113 (2002), and take the messenger mass scale $M_M = 2\Lambda$, $\tan(\beta) = 15$, $\mathrm{sgn}(\mu) = 1$, and the number of messenger fields $N_M = 1$. The parameters c_{Grav} (gravitino mass factor) and Λ (supersymmetry breaking scale) are allowed to vary.

[16] T. Sjöstrand, L. Lönnblad, and S. Mrenna, hep-ph/0108264. We used version 6.158 and use only leading order production cross sections to be conservative.

[17] F. Paige and S. Protopopescu, BNL Report No. BNL38034, 1986; F. Paige, S. Protopopescu, H. Baer, and X. Tata, hep-ph/0001086. We used version 7.64 to generate the SUSY masses.

[18] J. Conway, ''Pretty Good Simulation'' (PGS), http://www.physics.rutgers.edu/jconway/research/software/pgs/pgs.html. We used version 3.21. The CDF detector is described as a cylinder, with length 3.5 m and radius 1.7 m.

[19] E. Boos, A. Vologdin, D. Toback, and J. Gaspard, Phys. Rev. D **66**, 013011 (2002). We use Eq. 3 therein.

[20] Following Ref. [3], we have neglected the contribution from cosmic ray backgrounds. The probability of an event with a real photon and a fake photon from a cosmic ray is small, and can be removed with simple topology cuts with very high efficiency. Similar arguments hold for the case of two fake photons from cosmic ray background sources which is even more unlikely.

[21] Following [11], we have neglected the contribution from cosmic ray backgrounds. The probability of an event with two jets overlapping with a photon from a cosmic ray is small, and might be removed by requiring events where the photon is equal in magnitude and opposite in ϕ of the $\not{E}_T$.

[22] R. Culbertson *et al.*, hep-ph/0008070 (especially Fig. 18 therein).

[23] L. Balka *et al.*, Nucl. Instrum. Methods Phys. Res., Sect. A **267**, 272 (1988); CDF Collaboration, F. Abe *et al.*, Phys. Rev. Lett. **73**, 2662 (1994); D. Partos, Ph.D. thesis, Brandeis University, 2001.

[24] K. Hagiwara *et al.*, Phys. Rev. D **66**, 010001 (2002).

[25] Note that Fig. 14 shows the ALEPH exclusion for this GMSB model line instead of the exclusion from the general scan in [13]. Comparison shows that there is no visible difference.